Journal of the Brazilian Society of Mechanical Sciences and Engineering (2019) 41:260
https://doi.org/10.1007/s40430-019-1762-3

TECHNICAL PAPER

Finite Volume Monte Carlo (FVMC) method for the analysis of conduction heat transfer

Hooman Naeimi[1] · **Farshad Kowsary**[2]

Received: 24 October 2018 / Accepted: 13 May 2019 / Published online: 22 May 2019

Abstract

The numerical solution of the heat equation is a particularly challenging subject in complex, practical applications such as functionally graded materials for which analytical solution is not available or hardly attainable. The Monte Carlo method is a powerful technique with some advantages compared to the conventional methods and is often used when all else fail. In this paper, we introduce the Finite Volume Monte Carlo (FVMC) method for solving 3D steady-state heat equation where, instead of using the usual finite difference scheme for discretization of the heat equation, the finite volume scheme is used. The FVMC method is tested for three problems to assess the robustness of the method, first one in a simple geometry for validation and evaluation of the predictive performance, the second one in a complex geometry with unstructured mesh and the last one in a problem with a variable heat source and different kinds of boundary conditions. Comparisons were made to the analytical solution in the first test case, whereas for the remaining test cases, the CFD methods were utilized in the absence of the analytical solutions. It was observed that the FVMC temperature distribution agrees perfectly with analytical and CFD solutions in all problems. Despite expecting computational accuracy to improve by increasing total number of particles in the FVMC method, a very good accuracy was obtained for all considered problems after a small number of walks, and the calculated relative root-mean-square errors were below 1%.

Keywords Monte Carlo · Conduction · Heat transfer · Finite volume · Numerical simulation

List of symbols

A	Cross-sectional area (m^2)
C	Nondimensional temperature coefficient
a, b and c	Length, width and height of the box (m)
$\dot{E}$	Energy (W)
FVMC	Finite Volume Monte Carlo
g	Volumetric rate of internal energy generation (W/m^3)
$\bar{g}$	Average value of the volumetric rate of internal energy generation (W/m^3)
g_0	Heat generation coefficient (W/m^3)
k	Thermal conductivity (W/m K)
m_i	Total number of steps for each particle before reaching the boundary
N	Total number of particles
q	Heat flow rate (W)
R	Random number
S	Source term (W)
T	Temperature (K)
V	Volume (m^3)
x, y, z	Cartesian coordinates (m)

Greek letters

β, γ, η	Eigen values of the heat equation

1 Introduction

The modeling of the conduction heat transfer has gained significant importance in many engineering applications such as multilayer thermal insulators, composite materials and functionally graded materials (FGM) [1–3]. Unfortunately, most practical applications are complex involving variable thermophysical properties, three-dimensional geometries with arbitrarily shaped boundaries as well as complicated

Technical Editor: Francis HR Franca, Ph.D..

✉ Hooman Naeimi
h.naeimi@ub.ac.ir

[1] Department of Mechanical Engineering, University of Bojnord, P.O. Box 9453155111, Bojnord, North Khorasan, Iran

[2] School of Mechanical Engineering, College of Engineering, University of Tehran, Tehran, Iran

boundary conditions. As a result, the analytic solutions of the most heat conduction problems are difficult to obtain, if not impossible. The Monte Carlo method has long been recognized as a powerful tool for the solution of the heat equation as the governing equation of the heat conduction. During the early days of the Monte Carlo method, it was a time-consuming approach to produce accurate results compared to other numerical methods. The past few years have seen tremendous technological developments of processing speed, product price and memory capacity, and many researches have been conducted on the optimization of the Monte Carlo method which evolved the Monte Carlo method from a highly expensive tool to a more cost-effective algorithm for most science and engineering applications [4–7].

The Monte Carlo method was first applied by Haji-Sheikh and Sparrow [8] in the solution of heat conduction problems by using the finite difference scheme. The floating random walk concept was also introduced in their work to provide more flexibility to handle different problems. Kowsary and Arabi [9] used an appropriate coordinate transformation to obtain nondimensional heat equation and calculate temperature distribution for a simple two-dimensional anisotropic solid by using the finite difference form of the Monte Carlo method. They showed that significant reduction in process time may be attained by selection of suitable grid size. The application of the fixed-step Monte Carlo method in transient anisotropic heat conduction problems was considered by Kowsary and Irano [10] in a square geometry by first using the coordinate transformation and then using the finite difference method to discretize the heat equation. Grigoriu [11] developed a Monte Carlo method based on Itô process that could solve the transient and steady-state heat equations involving both Dirichlet and Neumann boundary conditions without any necessity to discretize the solution domain.

A new Monte Carlo method was applied by Wong et al. [12] to simulate phonon transport at nanoscales within silicon structures subjected to different heat sources by introducing a reference temperature. It was shown that the temperature distribution might be underestimated when an external heat generation term was considered in the governing heat equation. A mesh-free Monte Carlo method was proposed by Bahadori et al. [13] to investigate transient conductive heat transfer in multilayered composite materials. The proposed method was a combination of a transient Bessel function solution and steady-state peripheral integral method. The results of the method were verified by experimental data and FEM calculations. Hua and Cao [14] developed a two-step phonon tracing Monte Carlo method to simulate heat conduction in nanostructures. They calculated the effective thermal conductivities of three typical nanostructures by combining the initial and the internal phonon transmittances. The computational time of the proposed method was reported at least one order of magnitude less than that one for the standard Monte Carlo method, and the underprediction of the results was below 10%. In another research, semi-floating and full-floating random walk algorithms were proposed by Talebi et al. [15] to estimate the temperature distribution within five simple geometries. In the semi-floating random walk algorithm, the particle step size was assumed constant, whereas no limitations were considered for the direction of the particle motion. In the full-floating random walk, the step size varies and the direction is calculated randomly. The accuracy of both algorithms was verified by comparing the predictions to the finite difference results. The full-floating random walk algorithm was reported as the fastest approach in the steady-state conditions. It should be noted that the floating random walk methods may be so unstable in the immediate vicinity of the domain boundaries that increases the calculation time. In a practical application, Hua et al. [16] utilized the Monte Carlo method in combination with the simulated annealing algorithm to determine the thermal conductivity distribution of a modified concrete module as a thermal energy storage system. A piecewise function for the optimal distribution of the thermal conductivity was dependent on the amount of the high thermal conductivity additives and the ratio of thermal conductivities between the upper and lower boundaries of the concrete module. It is also appropriate to mention the recent application of the Monte Carlo method to solve inverse heat conduction problems that estimate unknown quantities appearing in the analysis of heat conduction problems based on the history of some heat flux and/or temperature measurements [17, 18]. For instance, an approximate Bayesian computation was used by Zeng et al. [19] in IHCP problems where in order to improve the efficiency of the method, a nonparametric population Monte Carlo was proposed together with fast computational techniques. They developed two heat conduction solvers for linear and nonlinear heat transfer problems. The linear solver was developed based on the superposition principle, whereas the reanalysis solver was recommended for the nonlinear problems, and they indicated good accuracy and efficiency in the considered benchmark problems.

For the solution of the heat equation by using the Monte Carlo method, an appropriate discretization technique to approximate all derivatives must be utilized. Among all the numerical discretization techniques, finite difference and finite volume are widely used to obtain a CFD solution of the heat equation. In all previous studies, the finite difference method was utilized by researchers to obtain a stochastic representation of the heat equation. Finite volume scheme has two advantages over the finite difference scheme, especially in complicated geometries, that justifies its application in the Monte Carlo method. First, this scheme ensures that energy is conserved

in the discretized cells. Second, in the finite volume method, a coordinate transformation to handle unstructured grid is no longer required.

Although solution of the heat equation has been studied extensively and there have been many papers on the subject, most of the researches have been limited to simple cases such as constant thermal properties, one or two-dimensional geometries, no internal heat generation or simple functional forms of thermal conductivities that simplify considerably the analysis of the heat conduction [20, 21]. The purpose of this article is to investigate the newly introduced Finite Volume Monte Carlo (FVMC) method for the solution of general steady-state heat equation without any limitations in the geometry, boundary conditions and physical properties. That is, the presented Finite Volume Monte Carlo approach provides great flexibility, in that a wide range of choices is available for the analysis of the conduction heat transfer. Thus, the FVMC method may be considered as a powerful statistical tool that spans a wide range of industrial and practical applications.

2 Mathematical description

The differential equation of heat conduction in general form, often called the heat equation, for a stationary, homogeneous, isotropic solid with heat generation within the body under steady-state conditions may be written as

$$\nabla \cdot (k\nabla T) + g = 0 \tag{1}$$

where ∇ is the three-dimensional del operator and g is the volumetric rate of internal energy generation. Performing integration over a control volume, which forms the key step of the finite volume method, results in the following expression:

$$\int_{\Delta V} \nabla \cdot (k\nabla T)\mathrm{d}V + \int_{\Delta V} g\mathrm{d}V = 0. \tag{2}$$

Using the divergence (Green's) theorem, the first volume integral in Eq. 2 is converted to surface integral, which provides an expression for the heat equation as

$$\int_{A} n \cdot (k\nabla T)\mathrm{d}A + \int_{\Delta V} g\mathrm{d}V = 0. \tag{3}$$

This integral form of the heat equation is applied to the domain of solution, which is divided into small volumes as elementary cells of the finite volume method. For a typical three-dimensional finite volume cell, shown in Fig. 1, omitting the surface-integral operation yields:

$$k_{\mathrm{e}}A_{\mathrm{e}}\left(\frac{\partial T}{\partial x}\right)_{\mathrm{e}} - k_{\mathrm{w}}A_{\mathrm{w}}\left(\frac{\partial T}{\partial x}\right)_{\mathrm{w}} + k_{\mathrm{n}}A_{\mathrm{n}}\left(\frac{\partial T}{\partial y}\right)_{\mathrm{n}} - k_{\mathrm{s}}A_{\mathrm{s}}\left(\frac{\partial T}{\partial y}\right)_{\mathrm{s}} + k_{\mathrm{t}}A_{\mathrm{t}}\left(\frac{\partial T}{\partial z}\right)_{\mathrm{t}} - k_{\mathrm{b}}A_{\mathrm{b}}\left(\frac{\partial T}{\partial z}\right)_{\mathrm{b}} + \bar{g}\Delta V = 0 \tag{4}$$

Here, $\bar{g}$ is the average value of the volumetric rate of internal energy generation, A is the cross-sectional area of the relevant control surface and ΔV is the volume. It is evident from Eq. 4 that the finite volume discretized heat equation has a clear physical interpretation. Equation 4 states that the heat transfer rate leaving the control volume minus the heat transfer rate entering to the control volume is equal to the internal energy generation, i.e., it constitutes an energy balance equation over the control volume.

$$\dot{E}_{\mathrm{in}} - \dot{E}_{\mathrm{out}} + \dot{E}_{g} = 0. \tag{5}$$

Thus, in the energy balance method, the finite volume form of the heat equation for a node may be obtained by applying conservation of energy to a control volume centered at that node. Since the actual direction of heat flow (inward or outward) is often unknown, it is convenient to formulate the energy balance by assuming that the heat flow is outward for the faces with positive normal vectors and the heat flow is inward for the faces with negative normal

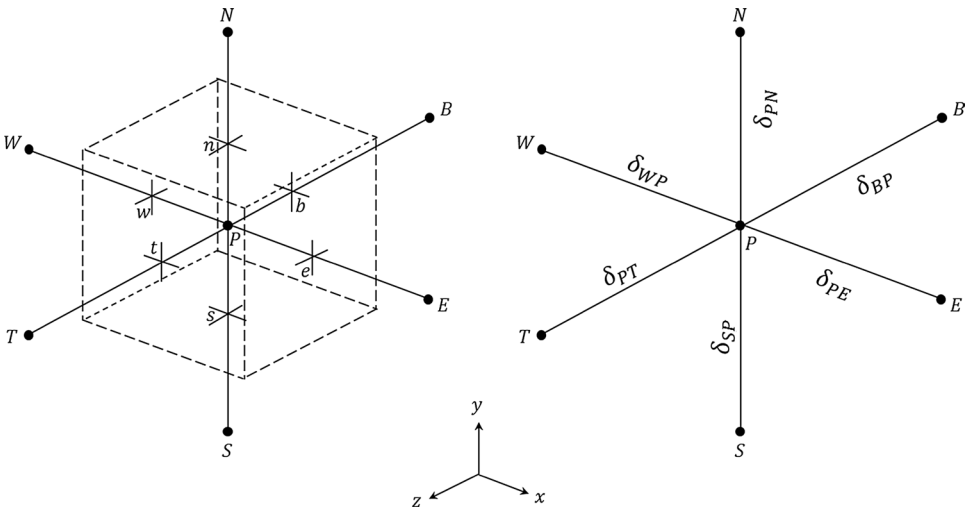

Fig. 1 A typical three-dimensional finite volume cell and neighboring nodes arrangement

vectors. For steady-state conditions with heat generation, the appropriate form of energy balance equation for the finite volume cell is depicted in Fig. 1, is

$$\left(q_{\mathrm{W}}+q_{\mathrm{S}}+q_{\mathrm{B}}\right)-\left(q_{\mathrm{E}}+q_{\mathrm{N}}+q_{\mathrm{T}}\right)+\bar{g}\Delta V=0. \tag{6}$$

As illustrated in Fig. 1, the general finite volume cell containing node P has six neighbors identified as east, west, north, south, top and bottom nodes (E, W, N, S, T, and B). Also, the notation e, w, n, s, t, and b are, respectively, used to refer the east, west, north, south, top and bottom cell faces. The interface thermal conductivity k along cell face in a uniform grid is calculated by linear interpolation between two adjacent nodes. The linearly interpolated values of k_{e}, k_{w}, k_{n}, k_{s}, k_{t} and k_{b} are given by

$$\begin{aligned} k_{\mathrm{e}}&=\frac{k_{\mathrm{E}}+k_{\mathrm{P}}}{2}, \quad k_{\mathrm{w}}=\frac{k_{\mathrm{W}}+k_{\mathrm{P}}}{2}, \quad k_{\mathrm{n}}=\frac{k_{\mathrm{N}}+k_{\mathrm{P}}}{2},\\ k_{\mathrm{s}}&=\frac{k_{\mathrm{S}}+k_{\mathrm{P}}}{2}, \quad k_{\mathrm{t}}=\frac{k_{\mathrm{T}}+k_{\mathrm{P}}}{2}, \quad k_{\mathrm{b}}=\frac{k_{\mathrm{B}}+k_{\mathrm{P}}}{2}. \end{aligned} \tag{7}$$

The temperature gradients along six cell faces may, in turn, be expressed as a function of the two adjacent nodal temperatures as

$$\begin{aligned} \left(\frac{\partial T}{\partial x}\right)_{\mathrm{e}}&=\frac{\left(T_{\mathrm{E}}-T_{\mathrm{P}}\right)}{\delta_{\mathrm{PE}}}, \quad \left(\frac{\partial T}{\partial x}\right)_{\mathrm{w}}=\frac{\left(T_{\mathrm{P}}-T_{\mathrm{W}}\right)}{\delta_{\mathrm{WP}}},\\ \left(\frac{\partial T}{\partial y}\right)_{\mathrm{n}}&=\frac{\left(T_{\mathrm{N}}-T_{\mathrm{P}}\right)}{\delta_{\mathrm{PN}}}, \quad \left(\frac{\partial T}{\partial y}\right)_{\mathrm{s}}=\frac{\left(T_{\mathrm{P}}-T_{\mathrm{S}}\right)}{\delta_{\mathrm{SP}}},\\ \left(\frac{\partial T}{\partial z}\right)_{\mathrm{t}}&=\frac{\left(T_{\mathrm{T}}-T_{\mathrm{P}}\right)}{\delta_{\mathrm{PT}}}, \quad \left(\frac{\partial T}{\partial z}\right)_{\mathrm{b}}=\frac{\left(T_{\mathrm{P}}-T_{\mathrm{B}}\right)}{\delta_{\mathrm{BP}}}. \end{aligned} \tag{8}$$

Substituting Eqs. 7 and 8 into Eq. 4, the finite volume form for an interior node with heat generation can be arranged as

$$\frac{k_{\mathrm{e}}A_{\mathrm{e}}}{\delta_{\mathrm{PE}}}T_{\mathrm{E}}+\frac{k_{\mathrm{w}}A_{\mathrm{w}}}{\delta_{\mathrm{WP}}}T_{\mathrm{W}}+\frac{k_{\mathrm{n}}A_{\mathrm{n}}}{\delta_{\mathrm{PN}}}T_{\mathrm{N}}+\frac{k_{\mathrm{s}}A_{\mathrm{s}}}{\delta_{\mathrm{SP}}}T_{\mathrm{S}}+\frac{k_{\mathrm{t}}A_{\mathrm{t}}}{\delta_{\mathrm{PT}}}T_{\mathrm{T}}+\frac{k_{\mathrm{b}}A_{\mathrm{b}}}{\delta_{\mathrm{BP}}}T_{\mathrm{B}}+\bar{g}\Delta\mathrm{V}=\left(\frac{k_{\mathrm{e}}A_{\mathrm{e}}}{\delta_{\mathrm{PE}}}+\frac{k_{\mathrm{w}}A_{\mathrm{w}}}{\delta_{\mathrm{WP}}}+\frac{k_{\mathrm{n}}A_{\mathrm{n}}}{\delta_{\mathrm{PN}}}+\frac{k_{\mathrm{s}}A_{\mathrm{s}}}{\delta_{\mathrm{SP}}}+\frac{k_{\mathrm{t}}A_{\mathrm{t}}}{\delta_{\mathrm{PT}}}+\frac{k_{\mathrm{b}}A_{\mathrm{b}}}{\delta_{\mathrm{BP}}}\right)T_{\mathrm{P}}. \tag{9}$$

This equation may be recast as

$$a_{\mathrm{E}}T_{\mathrm{E}}+a_{\mathrm{W}}T_{\mathrm{W}}+a_{\mathrm{N}}T_{\mathrm{N}}+a_{\mathrm{S}}T_{\mathrm{S}}+a_{\mathrm{T}}T_{\mathrm{T}}+a_{\mathrm{B}}T_{\mathrm{B}}+\bar{g}\Delta\mathrm{V}=a_{\mathrm{P}}T_{\mathrm{P}}. \tag{10}$$

The coefficients of the discretized heat equation at interior node P are given in Table 1.

We may rearrange Eq. 10 by dividing it by a_{P} as

$$C_{\mathrm{E}}T_{\mathrm{E}}+C_{\mathrm{W}}T_{\mathrm{W}}+C_{\mathrm{N}}T_{\mathrm{N}}+C_{\mathrm{S}}T_{\mathrm{S}}+C_{\mathrm{T}}T_{\mathrm{T}}+C_{\mathrm{B}}T_{\mathrm{B}}+S=T_{\mathrm{P}} \tag{11}$$

where all nondimensional coefficients and the source term (S) are included in Table 2. From Table 2, it is evident that the sum of temperature coefficients is equal to unity.

A probabilistic interpretation may be given to Eq. 11. If a random walking particle is instantaneously at the node P, it has transient probabilities C_{E}, C_{W}, C_{N}, C_{S}, C_{T}, and C_{B} of moving from P to point E, W, N, S, T, and B, respectively. A means of determining which way the particle should move is to generate a random number, R, uniformly distributed in the interval (0, 1), $0<R<1$, and instruct the particle to walk as follows:

$$\begin{aligned} &P\rightarrow E \quad \text{if } 0<R<C_{\mathrm{E}},\\ &P\rightarrow W \quad \text{if } C_{\mathrm{E}}<R<C_{\mathrm{E}}+C_{\mathrm{W}},\\ &P\rightarrow N \quad \text{if } C_{\mathrm{E}}+C_{\mathrm{W}}<R<C_{\mathrm{E}}+C_{\mathrm{W}}+C_{\mathrm{N}},\\ &P\rightarrow S \quad \text{if } C_{\mathrm{E}}+C_{\mathrm{W}}+C_{\mathrm{N}}<R<C_{\mathrm{E}}+C_{\mathrm{W}}+C_{\mathrm{N}}+C_{\mathrm{S}},\\ &P\rightarrow T \quad \text{if } C_{\mathrm{E}}+C_{\mathrm{W}}+C_{\mathrm{N}}+C_{\mathrm{S}}<R<C_{\mathrm{E}}+C_{\mathrm{W}}+C_{\mathrm{N}}+C_{\mathrm{S}}+C_{\mathrm{T}},\\ &P\rightarrow B \quad \text{if } C_{\mathrm{E}}+C_{\mathrm{W}}+C_{\mathrm{N}}+C_{\mathrm{S}}+C_{\mathrm{T}}<R<1. \end{aligned} \tag{12}$$

To calculate the temperature at node P, a particle as a random walker is instructed to start walking from this point to one of its six neighbors. The particle traverses the grid from node to node until it reaches to one of the solution domain boundaries, and then, the walk is terminated. When it does, the prescribed temperature T_{C} at that boundary is recorded. Let the value of T_{C} after first walk termination be denoted by $T_{\mathrm{C}}(1)$ and the corresponding recorded value of T_{C} for a

Table 1 Coefficients of the discretized heat equation at interior node

a_{E}	a_{W}	a_{N}	a_{S}	a_{T}	a_{B}	a_{P}
$\frac{k_{\mathrm{e}}A_{\mathrm{e}}}{\delta_{\mathrm{PE}}}$	$\frac{k_{\mathrm{w}}A_{\mathrm{w}}}{\delta_{\mathrm{WP}}}$	$\frac{k_{\mathrm{n}}A_{\mathrm{n}}}{\delta_{\mathrm{PN}}}$	$\frac{k_{\mathrm{s}}A_{\mathrm{s}}}{\delta_{\mathrm{SP}}}$	$\frac{k_{\mathrm{t}}A_{\mathrm{t}}}{\delta_{\mathrm{PT}}}$	$\frac{k_{\mathrm{b}}A_{\mathrm{b}}}{\delta_{\mathrm{BP}}}$	$a_{\mathrm{E}}+a_{\mathrm{W}}+a_{\mathrm{N}}+a_{\mathrm{S}}+a_{\mathrm{T}}+a_{\mathrm{B}}$

Table 2 Coefficients of the rearranged heat equation at interior node

C_{E}	C_{W}	C_{N}	C_{S}	C_{T}	C_{B}	S
$\frac{a_{\mathrm{E}}}{a_{\mathrm{P}}}$	$\frac{a_{\mathrm{W}}}{a_{\mathrm{P}}}$	$\frac{a_{\mathrm{N}}}{a_{\mathrm{P}}}$	$\frac{a_{\mathrm{S}}}{a_{\mathrm{P}}}$	$\frac{a_{\mathrm{T}}}{a_{\mathrm{P}}}$	$\frac{a_{\mathrm{B}}}{a_{\mathrm{P}}}$	$\frac{1}{a_{\mathrm{P}}}\bar{g}\Delta\mathrm{V}$

second particle which is released from point P and reached to another boundary cell be denoted by $T_C(2)$, as depicted in Fig. 2 for a simple two-dimensional grid. After repeating this procedure for third, fourth, …, Nth particles released from the same point and recording corresponding prescribed temperatures as $T_C(3), T_C(4), \ldots, T_C(N)$, the temperature of node P may be calculated from the expected value of all recorded temperatures. For the general case of the heat equation, considering volumetric heat generation, the term $\bar{g}\Delta V/a_P$ must be recorded at every step of particle random walk. Therefore, the temperature of interior node P may be given by

$$T_P = \frac{1}{N}\sum_{i=1}^{N} T_C(i) + \frac{1}{N}\sum_{i=1}^{N}\sum_{j=1}^{m_i-1}\frac{\Delta V}{a_P}\bar{g}(x_j, y_j, z_j) \tag{13}$$

where N is the total number of walks and m_i is the total number of steps for ith random particle released from point P to reach the boundary. The iterative procedure of the FVMC method to solve the heat equation is shown as a flowchart in Fig. 3.

For each nodal point at which the temperature is unknown, an appropriate FVMC relation must be developed based on the energy balance method in Eq. 6. The FVMC relation for a boundary cell exposed to convectional heat transfer with convectional coefficient h and reference fluid temperature T_∞, as shown in Figs. 4, is derived as

$$\begin{aligned} &a_W T_W + \frac{1}{2}a_N T_N + \frac{1}{2}a_S T_S + \frac{1}{2}a_T T_T \\ &\quad + \frac{1}{2}a_B T_B + hA_e T_\infty + \bar{g}\Delta V \\ &\quad = \left(a_W + \frac{1}{2}a_N + \frac{1}{2}a_S + \frac{1}{2}a_T + \frac{1}{2}a_B + hA_e\right)T_P. \end{aligned} \tag{14}$$

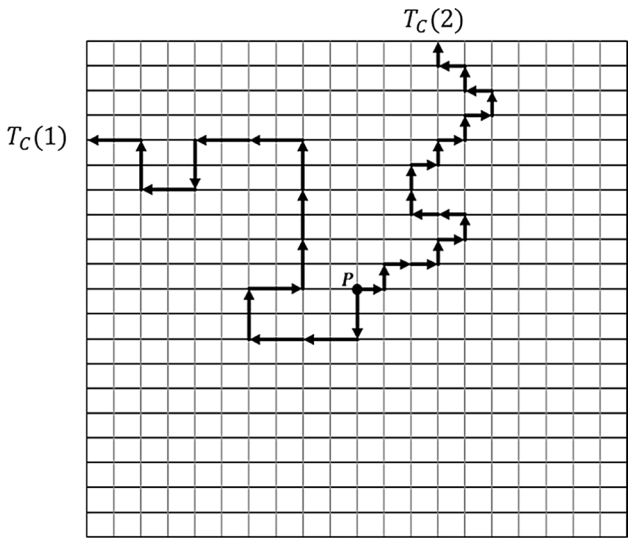

Fig. 2 Traversed path for two random particles from point P to domain boundaries

The energy balance method is used in a similar manner to obtain the heat equation for a boundary cell subjected to uniform heat flux at a plane, as shown in Fig. 5. The FVMC form of heat equation is presented in Eq. 15.

$$\begin{aligned} &a_W T_W + \frac{1}{2}a_N T_N + \frac{1}{2}a_S T_S + \frac{1}{2}a_T T_T \\ &\quad + \frac{1}{2}a_B T_B + q'' A_e + \bar{g}\Delta V \\ &\quad = \left(a_W + \frac{1}{2}a_N + \frac{1}{2}a_S + \frac{1}{2}a_T + \frac{1}{2}a_B\right)T_P. \end{aligned} \tag{15}$$

The temperature coefficients, a_E, a_W, a_N, a_S, a_T and a_B, are the same as the ones obtained for Eq. 10, as presented in Table 1.

The FVMC method owes much of its flexibility to the fact that spatial discretization is totally flexible for using unstructured meshes which is of interest in most practical applications. Random walk probabilities for an unstructured finite volume cell, as shown in Fig. 6, may be determined using the energy balance method. By using the energy balance method, the FVMC relation for a nodal point in an unstructured mesh is written as

$$C_E T_E + C_W T_W + C_S T_S + C_B T_B + S = T_P. \tag{16}$$

Again, temperature coefficients and source term are defined exactly as in Table 1.

One important advantage of the FVMC method is that it can be applied to the variable thermal conductivity problems in a noninvasive manner, in which the thermal conductivity is a function of the spatial coordinates or where it is a discontinuous function such as multilayer bodies. It means that there is no need for thermal conductivity to be differentiable everywhere which covers a larger class of problems that can be analyzed by the FVMC method without any necessity to calculate thermal conductivity gradients similar to the one calculated in the finite difference method. The other attribute of the FVMC method which is clear from Eq. 4 is that it can be easily utilized for problems with boundary conditions of the second and third kinds without any necessity to calculate temperature gradients at the boundary faces of the boundary control volumes.

3 Results and discussion

The FVMC method developed in this study will be checked for its validity by comparison with data of analytical formula and CFD method. Three different problems are investigated in this section to show the performance of the FVMC method. As a first example, the FVMC method was applied to a problem, in which its analytical solution is available to indicate the prediction performance of the method. Next, it

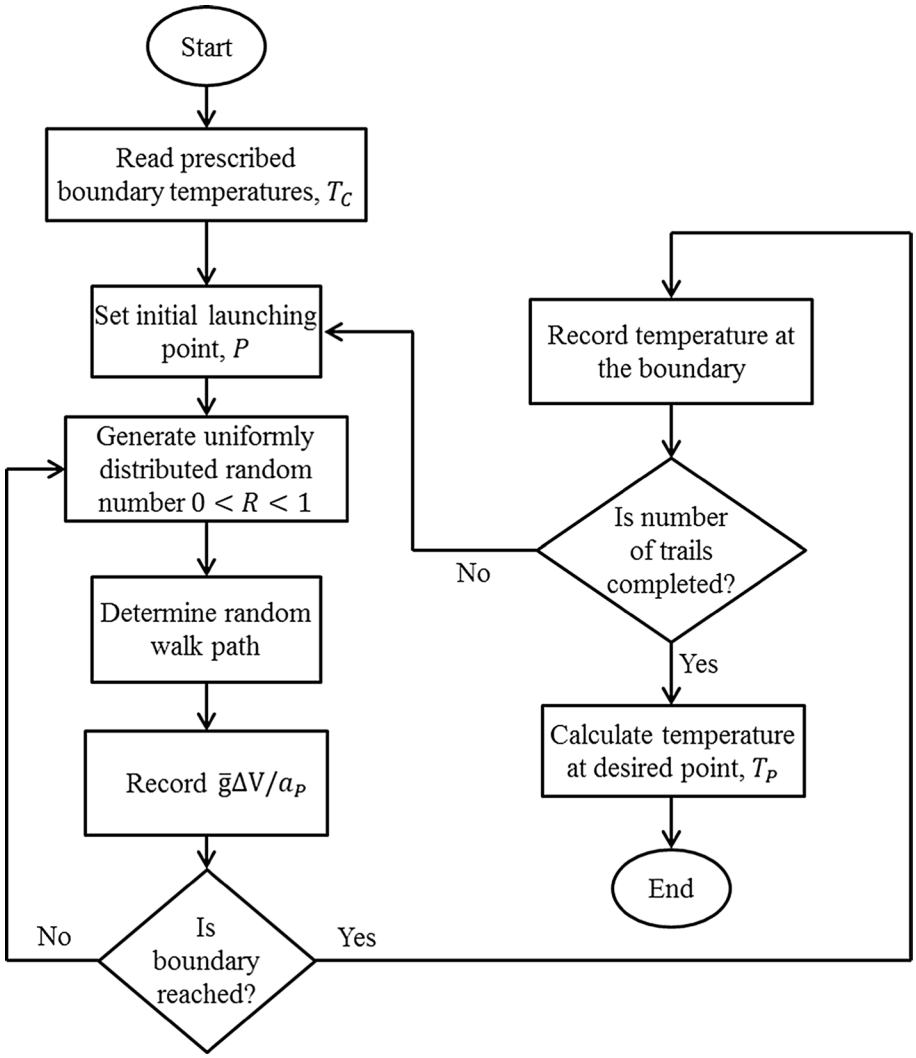

Fig. 3 Flowchart of FVMC method

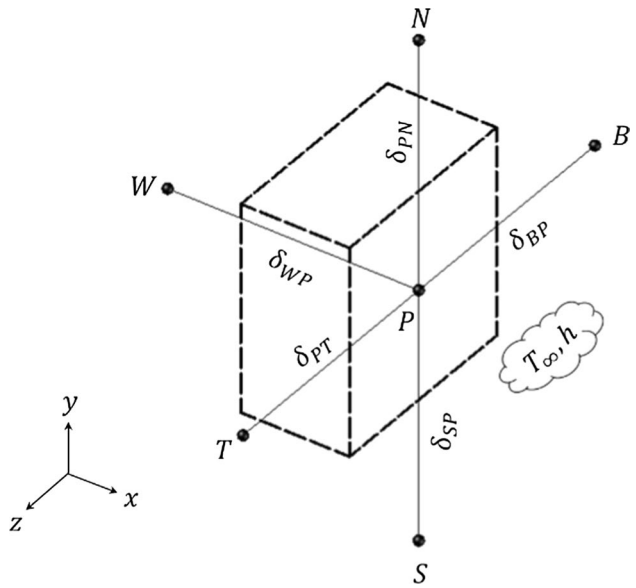

Fig. 4 Boundary cell with convection at a plane surface

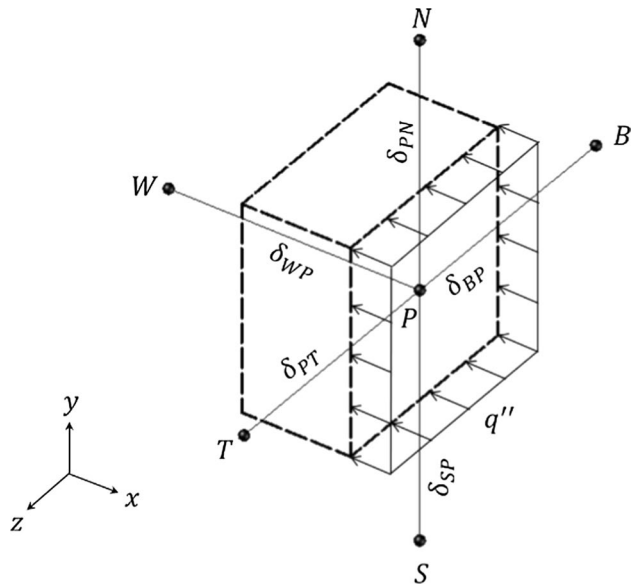

Fig. 5 Boundary cell with uniform heat flux at a plane surface

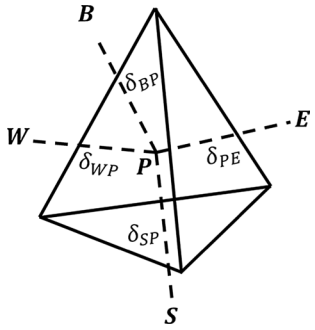

Fig. 6 A typical tetrahedron finite volume cell

was used in a complex geometry with unstructured mesh and finally, it was used in a problem with different kinds of boundary conditions where a variable heat source is present within the medium.

3.1 Solid box with uniform heat generation

The performance of the FVMC method cannot be assessed unless the results are compared with the analytical solution. In this section, the FVMC method was verified by comparing results against analytically calculated temperatures. The test case considered here for verification is that of conduction heat flow in a three-dimensional solid box with zero surface temperature, uniform heat source and constant thermal conductivity. From Hahn and Özişik [22], the steady-state temperature distribution within a rectangular parallelepiped is given by:

$$T_{ss}(x,y,z) = \frac{64}{abc}\frac{g_0}{k}\sum_{m\ \text{odd}}^{\infty}\sum_{n\ \text{odd}}^{\infty}\sum_{p\ \text{odd}}^{\infty} \frac{1}{\eta_p\gamma_n\beta_m\left(\beta_m^2+\gamma_n^2+\eta_p^2\right)}\sin\beta_m x\sin\gamma_n y\sin\eta_p z \tag{17}$$

where g_0 is the uniform heat generation, k is the constant value of thermal conductivity of the solid and a, b, and c are the length, width and height of the box, respectively. The eigenvalues of β_m, γ_n and η_p may also be expressed as

$$\beta_m = \frac{m\pi}{a},\quad \gamma_n = \frac{n\pi}{b},\quad \eta_p = \frac{p\pi}{c},\quad \text{with } (m,n,p) = 1,3,5,\ldots \tag{18}$$

Temperature field in the form of isotherms for the considered test case was obtained using the FVMC method on the mid-plane of the geometry ($z = 0.5m$) and presented along with the temperature contour of the analytical solution of Eq. 17 on the same plane in Fig. 7a, b, respectively. For simplicity, all calculations were performed on a unit cube with $a = b = c = 1$ m and $g_0 = 1000$ W/m^3. Due to symmetry,

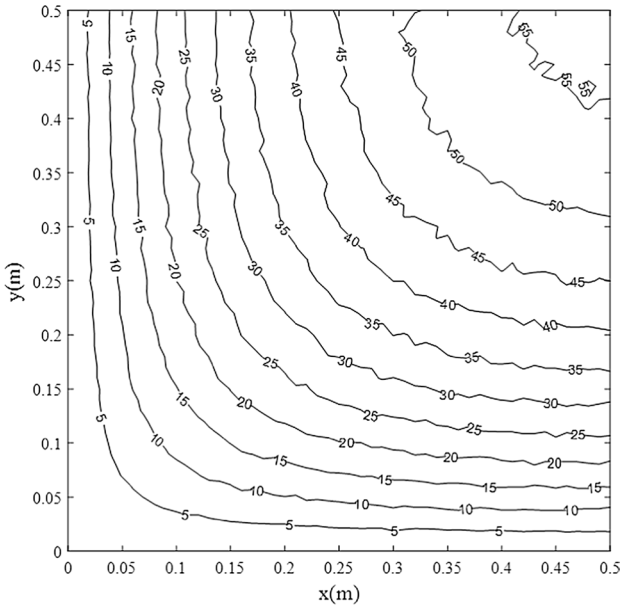

(a) FVMC prediction

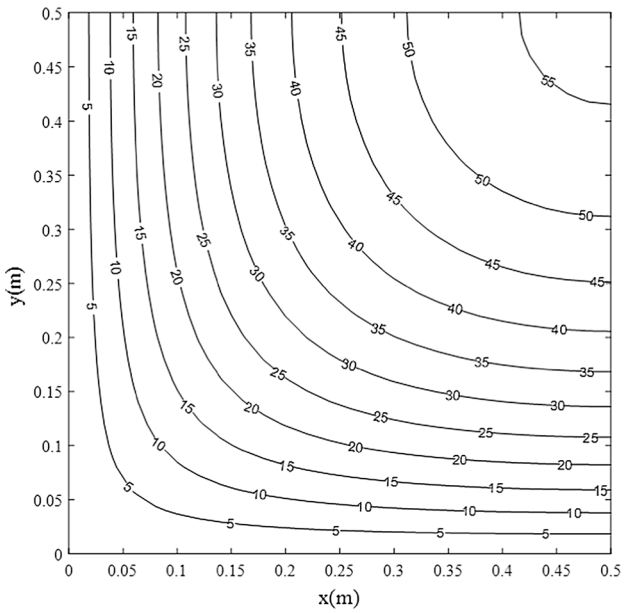

(b) Analytical solution

Fig. 7 Temperature contour of the box with uniform generation on the $z = 0.5m$ plane

only a quarter of the solution domain is drawn in Fig. 7a, b. As evident by comparing Fig. 7a, b, the FVMC predictions are in good agreement with analytical data.

The relative root-mean-square error, e_{rms}, gives a better understanding of the FVMC predictions in terms of the total number of random walks. The relative root-mean-square error quantifies the difference between exact and estimated results defined as

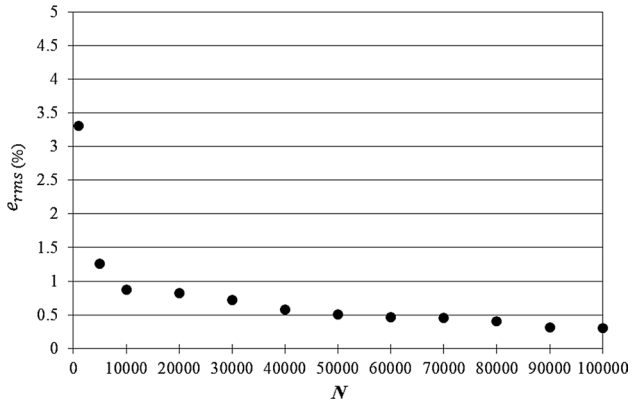

Fig. 8 e_{rms} of the FVMC results on the $z = 0.5$ m plane for the solid box with uniform heat generation

$$e_{\text{rms}} = \sqrt{\frac{1}{n_x}\sum_{i=1}^{n_x}\left(\frac{T_{i,\text{FVMC}} - T_{i,\text{anal}}}{T_{i,\text{anal}}} \times 100\right)^2} \tag{19}$$

where $T_{i,\text{FVMC}}$ is the estimated temperature from the FVMC method at place i, $T_{i,\text{anal}}$ is the calculated value from Eq. 17 at the same point and n_x is the number of intervals along the x-axes on the midline of the $z = 0.5$ m plane. The relative root-mean-square error for various values of random walks, N, computed by the FVMC method is shown in Fig. 8. The most striking feature of Fig. 8 is the steep reduction trend of e_{rms} for increasing N, at the beginning of the range. This fact means that by using relatively small N (e.g., 10,000), the computed e_{rms} of the FVMC results is less than about 1%.

3.2 Three-dimensional L-shaped body with variable thermal conductivity

As explained in Sect. 2, the FVMC method is more advantageous in case of using an unstructured mesh that makes it much more efficient for analyzing complex problems. Following verification of the FVMC method, studies were undertaken to judge the effectiveness of the method in an L-shaped body as shown in Fig. 9. Consider the case of constant heat generation in the medium $g_0 = 50,000$ W/m^3, in which the thermal conductivity is assumed to be an exponential function of x, y and z directions as

$$k = k_0 \exp(x) \exp(2y) \exp(4z) \tag{20}$$

where $k_0 = 1$ W/m K and the boundary surface of the cylindrical holes are kept at a constant temperature of 200 °C, while all other surfaces are maintained at zero temperature.

For the unstructured mesh shown in Fig. 9, random walk probabilities may be calculated using the energy balance method as described for a tetrahedron cell of Fig. 6. In order

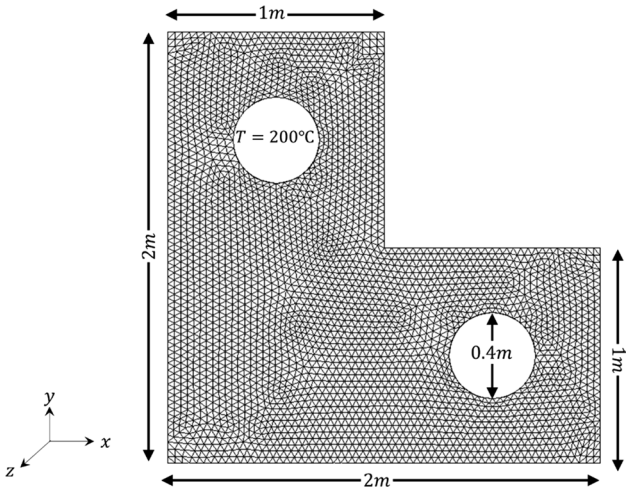

Fig. 9 L-shaped body with unstructured mesh

to give better insight into the accuracy of the FVMC method, it may be useful to compute the temperature distribution over the mid-plane of the geometry ($z = 0.5$ m) and compare the results with those of CFD code. The FVMC and CFD results are plotted as a contour plot in Fig. 10a, b, respectively. Comparison of these figures reveals that FVMC results are perfectly consistent with CFD results, and all predicted temperature levels are nearly in exact agreement with the values obtained using the CFD method where the differences are not clearly visible.

3.3 Unit cube with variable heat source and different boundary conditions

The FVMC method is now subjected to different kinds of boundary conditions. The test case considered here is a unit cube with constant thermal conductivity $k = 200$ W/m K where a sinusoidal heat source is presented within the body as:

$$g = 10^5 \sin(\pi x) \sin(\pi y) \sin(\pi z). \tag{21}$$

The temperatures of the north and south walls are varying with x and y directions as:

$$T_{n,s} = 200 \sin(\pi x) \sin(\pi y), \tag{22}$$

while the back and top surfaces are insulated and the west and east surfaces dissipate heat by convection with a heat transfer coefficient $h = 100$ W/m^2 K into a fluid of temperature $T_\infty = 25$ °C. As can be deduced from Eq. (15), an insulated surface $\left(q'' = 0\right)$ may be treated as reflecting barrier. Also, the random walk probabilities for a boundary node in the convective boundary condition are calculated from Eq. 14. Computations were performed using both the FVMC and CFD methods. Figure 11a, b shows the computed

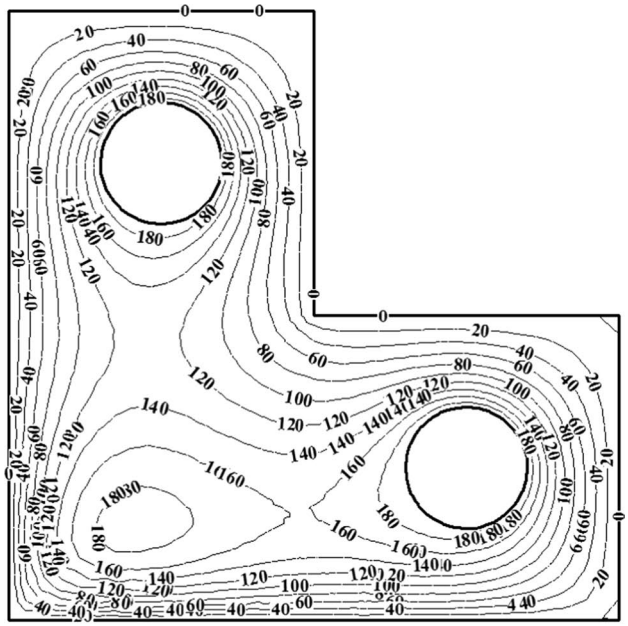

(a) FVMC prediction

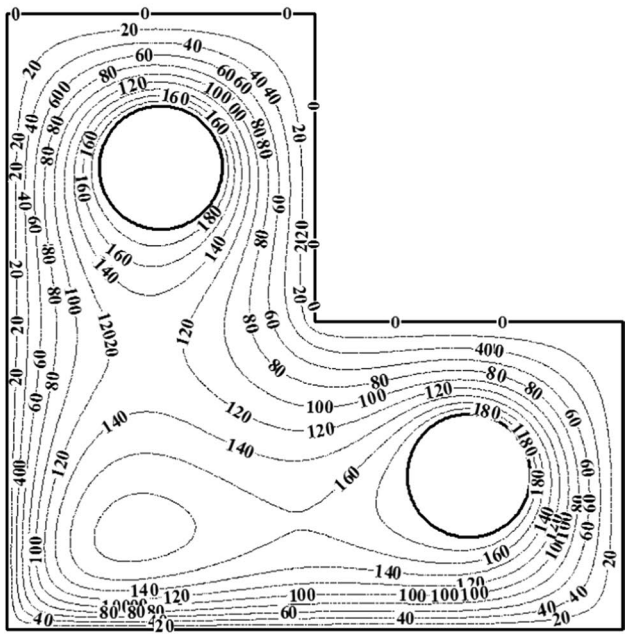

(b) CFD solution

Fig. 10 Temperature contour of the L-shaped body with uniform generation and variable thermal conductivity on the $z = 0.5m$ plane

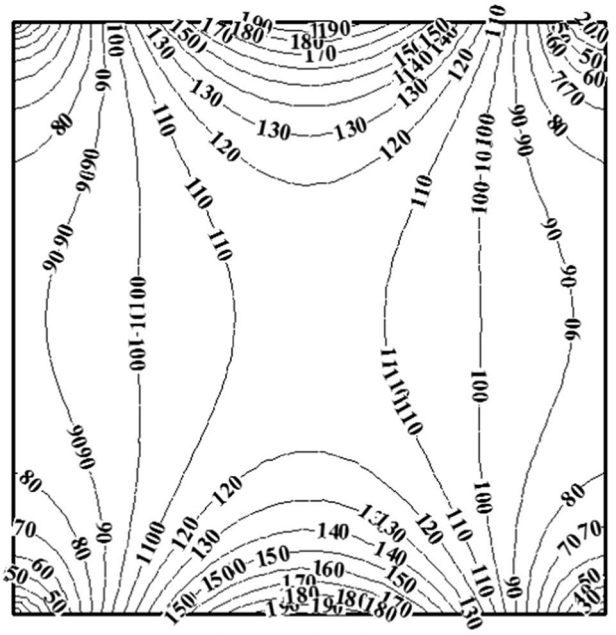

(a) FVMC prediction

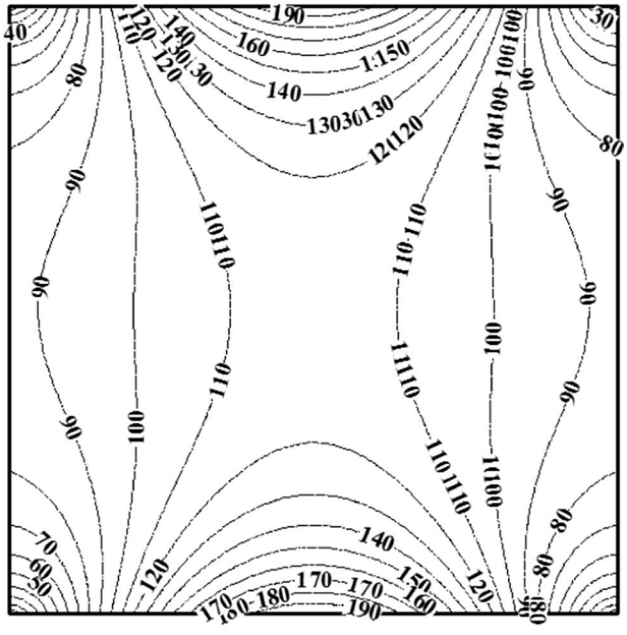

(b) CFD solution

Fig. 11 Temperature contour of the unit cube with different boundary conditions on the $x = 0.5$ plane

temperature distribution on the $x = 0.5$ m plane from the FVMC method and the CFD code, respectively. It can be seen that these two sets of results agree very well which means that the FVMC method can predict the temperature distribution in the case of using different kinds of boundary conditions.

4 Conclusion

In this paper, we have introduced the FVMC method to solve the general steady-state heat equation. Our simulations were conducted in three test cases with different levels of complexity to illustrate the general applicability of this method. Since the analytical solutions of the last two test cases are not available, the CFD solution in the same

Table 3 Relative root-mean-square error, e_{rms}, for all considered test cases

$e_{\text{rms}}(\%)$		
Test case 1	Test case 2	Test case 3
0.895	0.774	0.543

grid network was used to calculate the e_{rms} error, in which the results are reported in Table 3 along with the one calculated for the first problem for $N = 100,000$. As can be seen in Table 3, the FVMC method can be considered as a precise estimator in the analysis of the conduction heat transfer problems.

Based on the three test cases considered in this paper, the following conclusions may be drawn:

- The FVMC simulation results were compared with those from the analytical formula and CFD solutions, and good agreement was observed.
- Despite the theoretical dependency of the FVMC results to the number of walks, it was demonstrated that a very good accuracy may be obtained after a certain number of walks, i.e., $N = 10,000$ that is not a big number for most numerical simulations.
- The FVMC method is easy to implement. It does not rely heavily on mathematical operations such as matrix inversion or iterative methods for solving the system of equations to compute unknown temperatures that require the assistance of an expert.
- The FVMC basic relation is simple to develop by using the energy balance method for each kind of cells or boundary conditions, allowing one to solve problems with complicated solution regions.
- The FVMC method ensures conservation of energy in the solution domain and may be used on an unstructured grid without any transformation.
- Unlike other conventional solution methods like finite difference, there is no need to save the temperature coefficient matrix for the entire grid, and the computer code does not require large memory even for multidimensional problems. All that is needed for the FVMC method is the calculation of the transient probabilities, that is, done simply during the grid traversal.
- The FVMC method is quite suitable for problems that need to obtain the temperature directly at one or several arbitrary points without the whole field computation.

References

1. Noda N (1999) Thermal stresses in functionally graded materials. J Therm Stresses 22(4–5):477–512
2. Gallegos-Muñoz A, Violante-Cruz C, Balderas B, Rangel-Hernandez V, Belman-Flores J (2010) Analysis of the conjugate heat transfer in a multi-layer wall including an air layer. Appl Therm Eng 30:599–604
3. Norouzi M, Rahman H, Birjandi A, Jone A (2016) A general exact analytical solution for anisotropic non-axisymmetric heat conduction in composite cylindrical shells. Int J Heat Mass Transf 93:41–56
4. Howell J (1998) The Monte Carlo method in radiative heat transfer. J Heat Transf Trans ASME 120:547–560
5. Naeimi H, Kowsary F (2017) An optimized and accurate Monte Carlo method to simulate 3D complex radiative enclosures. Int Commun Heat Mass Trans 84:150–157
6. Naeimi H, Kowsary F (2017) Macro-voxel algorithm for adaptive grid generation to accelerate grid traversal in the radiative heat transfer analysis via Monte Carlo method. Int Commun Heat Mass Trans 87:22–29
7. Sadiku MNO (2009) Monte Carlo methods for electromagnetics. CRC Press, Boca Raton
8. Haji-Sheikh A, Sparrow E (1967) The solution of heat conduction problems by probability methods. J Heat Transf Trans ASME 89:121–130
9. Kowsary F, Arabi M (1999) Monte Carlo solution of anisotropic heat conduction. Int Commun Heat Mass Transf 26(8):1163–1173
10. Kowsary F, Irano S (2006) Monte Carlo solution of transient heat conduction in anisotropic media. J Thermophys Heat Transf 20(2):342–345
11. Grigoriu M (2000) A Monte Carlo solution of heat conduction and Poisson equations. J Heat Transf Trans ASME 122:40–45
12. Wong B, Francoeur M, Pinar Mengüç M (2011) A Monte Carlo simulation for phonon transport within silicon structures at nanoscales with heat generation. Int J Heat Mass Transf 54:1825–1838
13. Bahadori R, Gutierrez H, Manikonda Sh, Meinke R (2018) A mesh-free Monte-Carlo method for simulation of three-dimensional transient heat conduction in a composite layered material with temperature dependent thermal properties. Int J Heat Mass Transf 119:533–541
14. Hua Y-C, Cao B-Y (2017) An efficient two-step Monte Carlo method for heat conduction in nanostructures. J Comput Phys 342:253–266
15. Talebi S, Gharehbash K, Jalali HR (2017) Study on random walk and its application to solution of heat conduction equation by Monte Carlo method. Prog Nucl Energy 96:18–35
16. Hua Y-C, Zhao T, Gua Z-Y (2017) Transient thermal conduction optimization for solid sensible heat thermal energy storage modules by the Monte Carlo method. Energy 133(C):338–347
17. Haji-Sheikh A, Buckingham F (1993) Multidimensional inverse heat conduction using the Monte Carlo method. J Heat Transf Trans ASME 115:26–33
18. Woodbury K, Beck J (2013) Estimation metrics and optimal regularization in a Tikhonov digital filter for the inverse heat conduction problem. Int J Heat Mass Transf 62:31–39
19. Zeng Y, Wang H, Zhang S, Cai Y, Li E (2019) A novel adaptive approximate Bayesian computation method for inverse heat conduction problem. Int J Heat Mass Transf 134:185–197
20. Ohmichi M, Noda N, Sumi N (2017) Plane heat conduction problems in functionallygraded orthotropic materials. J Therm Stresses 40(6):747–764
21. Hsueh-Hsien LuH, Young D, Sladek J, Sladek V (2017) Three-dimensional analysis for functionally graded piezoelectric semiconductors. J Intell Mater Syst Struct 28(11):1391–1406
22. Hahn D, Özişik M (2012) Heat conduction. Wiley, Hoboken